47th AIAA/ASME/ASCE/AHS/ASC Structures, Structural Dynamics, and Materials Confere
1 - 4 May 2006, Newport, Rhode Island

AIAA 2006-1848

Suppression of Aeroelastic Instability with a Nonlinear Energy Sink: Experimental Results

W. Joel Hill[*], Thomas W. Strganac[†], and Chetan Nichkawde[*]
Texas A&M University, College Station, Texas, 77843

D. Michael McFarland[‡], Gaetan Kerschen[§], Young S. Lee[¶], Alexander F. Vakakis[#], and Lawrence A. Bergman[**]
University of Illinois at Urbana-Champaign, Urbana, Illinois, 61801

The presence of limit cycle oscillations within the flight envelopes of existing aircraft is well documented. Future air vehicle designs are also likely to encounter limit cycle oscillations under certain loading conditions. These steady-state constant amplitude oscillations are detrimental to mission effectiveness and lead to increased fatigue of aircraft structures. Previous efforts to suppress limit cycle oscillations have focused primarily on active control methods. These efforts have been effective but require significant measurement and control resources. In this study the investigators test a passive method for suppressing limit cycle behavior. A nonlinear energy sink, based on the principle of nonlinear energy pumping, is shown to be effective for increasing the stability threshold of a nonlinear two degree of freedom aeroelastic system.

Nomenclature

α	=	pitch displacement
a	=	wing elastic axis location non-dimensionalized by wing semichord
b	=	wing semichord
c_α	=	viscous pitch damping coefficient
c_h	=	viscous plunge damping coefficient
c_s	=	NES viscous damping coefficient
F_c	=	Coulomb damping force
F_s	=	force exerted by the NES on the NATA
h	=	plunge displacement
I_α	=	mass moment of inertia about the elastic axis of all rotating parts
k_α	=	pitch stiffness
k_h	=	plunge stiffness
k_s	=	NES nonlinear spring coefficient
L	=	aerodynamic lift force
M_α	=	aerodynamic moment about the elastic axis
M_c	=	Coulomb damping moment
m_c	=	mass of pitch cam
m_T	=	mass of entire plunging apparatus: wing, pitch cam, and plunge carriage
m_w	=	mass of wing section alone

[*] Graduate Research Assistant, Department of Aerospace Engineering, 3141 TAMU, Member, AIAA.
[†] Professor, Department of Aerospace Engineering, 3141 TAMU, Associate Fellow, AIAA.
[‡] Research Associate Professor, Department of Aerospace Engineering, MC-236, 104 S. Wright St., Senior Member, AIAA.
[§] Visiting Scholar, Department of Aerospace Engineering, MC-236, 104 S. Wright St.; currently Postdoctoral Researcher, Department of Material, Mechanical and Aerospace Engineering, University of Liege, Belgium.
[¶] Graduate Research Assistant, Department of Mechanical & Industrial Engineering, MC-244, 1206 W. Green St.
[#] Professor, National Technical University of Athens, Greece; Adjunct Professor, Department of Mechanical & Industrial Engineering and Department of Aerospace Engineering UIUC, MC-236, 104 S. Wright St.
[**] Professor, Department of Aerospace Engineering, MC-236, 104 S. Wright St., Associate Fellow, AIAA.

r_c = distance between pitch cam mass center and wing chord line
r_{cg} = distance between wing mass center and elastic axis
v = NES displacement

I. Introduction

Limit cycle oscillations (LCOs) occur with many different aircraft models. Denegri[1] and Bunton and Denegri[2] observed limit cycle oscillations in flight tests of the F-16 and F/A-18 when certain wing-mounted stores were present. Croft[3] has discussed limit cycle oscillations in the elevators of several Airbus passenger airplanes. Limit cycle oscillations lead to increased aircraft structural fatigue, limitations on flight performance, and an increase in workload for pilots.[4]

Many authors have studied the causes of limit cycle oscillations. The common factor in all aircraft systems exhibiting limit cycle behavior is aeroelastic nonlinearities. These nonlinearities can exist in the flow field, the structure, or both. Reference 4 provides an excellent summary of recent studies done in the fields of aerodynamics and structural dynamics to understand nonlinear aeroelasticity. Cunningham[5] and Hartwich et al.[6] examined nonlinear aerodynamics and the contributions these nonlinearities make to producing LCOs. Chen et al. [7] described the role of nonlinear structural damping in the development of LCOs. Gilliatt et al.[8] and Thompson and Strganac[9] examined the influence of internal resonance nonlinearities on LCO behavior.

Stiffness nonlinearity was examined by Tang and Dowell.[10] They described LCOs as the interaction of the nonlinear structure with nonlinear aerodynamics and provided experimental and theoretical results. Many analytical studies of nonlinear stiffness were performed by O'Neil[11], O'Neil et al.[12], Sheta et al.[13], and Thompson[14]. These studies were all experimentally validated using the nonlinear aeroelastic test apparatus (NATA) in a low-speed wind tunnel at Texas A&M University.

Many authors have also studied methods for controlling or suppressing limit cycle oscillations. Ko et al.[15,16] and Block and Strganac[17] developed several control laws using linear theory, partial feedback linearization, and adaptive control to stabilize an inherently unstable aeroelastic system with a single trailing edge control surface. Platanitis and Strganac[18] used feedback linearization and model reference adaptive control to stabilize an aeroelastic system with leading and trailing edge control surfaces. These authors have shown that active control can be used to raise the threshold velocity above which LCOs occur.

While active control has been shown to be effective in suppressing LCOs, these methods require significant use of control resources. Active methods also require sensors capable of constantly providing accurate measurements of the system state for feedback into the controller. Herein, we present results obtained using nonlinear energy pumping to effectively suppress limit cycle oscillations in an unstable aeroelastic system. The nonlinear energy sink used to suppress the LCO is a completely passive device with no state measurement or control input required.

II. The Nonlinear Energy Sink and LCO Suppression

Nonlinear energy pumping refers to the irreversible transfer of vibration energy from the main structure of a dynamic system to an attachment with essentially nonlinear (nonlinearizable) stiffness and linear damping. Vakakis and Gendelman[19] and Vakakis et al.[20] showed that when the essentially nonlinear oscillator resonates with a mode of the main system, energy is transferred (pumped) from the main system to the nonlinear attachment irreversibly. The attachment thus acts as a nonlinear energy sink (NES).

The NES is a passive vibration controller that has been developed and studied at the University of Illinois at Urbana-Champaign[19-31] (UIUC). Unlike a linear dynamic absorber, which is effective in narrow frequency bands, the NES works against broadband distubances. In addition, while the linear absorber is a steady-state device, the NES provides transient protection as well.

The essentially nonlinear stiffness and damping in the NES make it possible to localize the energy from the primary system through resonance capture and to dissipate the transferred energy[19-21]. Recently, a two-degree-of-freedom nonlinear system consisting of a grounded linear oscillator coupled to an NES was studied to obtain the very complicated bifurcation structure of its nonlinear normal modes[22]. Furthermore, it was shown that there exist at least three mechanisms of energy pumping; namely, one-to-one and subharmonic resonance captures, and energy pumping initiated by nonlinear beating phenomena[23]. It was also shown that the transient dynamics and energy transfer can be systematically interpreted and understood by studying the topology and bifurcations of the periodic orbits of the underlying Hamiltonian system.

Lee et al.[24] showed the applicability of nonlinear energy pumping to suppress the LCO of a van der Pol (VDP) oscillator, which is analogous to a nonlinear aeroelastic problem. The LCO suppression mechanism was found to be a series of captures into, and escapes from, resonances, from superharmonic to subharmonic order.

Lee et al.[25] also studied triggering mechanisms of LCOs caused by the aeroelastic instability of a rigid wing with nonlinear stiffness in both heave and pitch. Their study was performed under conditions of subsonic flow assuming quasi-steady aerodynamics. They found that the LCO triggering mechanism consists of a combination of different dynamic phenomena, taking place in three main stages or regimes: attraction to transient resonance captures, escapes from these captures and, finally, entrapments into permanent resonance captures. The general conclusion was that an initial excitation of the heave mode by the flow acts as the triggering mechanism for the excitation of the pitch mode through nonlinear interactions resulting from the resonance captures and escapes. The eventual excitation of the pitch mode signifies the appearance of LCOs of the wing in flow.

A companion paper[26] to the present work shows that there exist three mechanisms for suppression of LCOs when applying a single-degree-of-freedom NES to the 2-DOF rigid wing in flow: (1) repeated burst-out and suppression; (2) intermediate suppression; and (3) complete suppression. The first mechanism turns out to determine critical boundaries for proper design of NES parameters. Furthermore, it is analytically shown that each suppression mechanism derives from similar behavior as in the case of LCO suppression of the VDP oscillator; that is, each is composed of a series of resonance captures and escapes from superharmonic to subharmonic order.

In this study, we adapted the NES developed at UIUC[27] to the two degree-of-freedom nonlinear aeroelastic test apparatus at Texas A&M University. The capacity of the NES to reduce or even eliminate these undesired oscillations and to extend the operating speed range of the system was conclusively verified.

III. Experimental Setup

The Nonlinear Aeroelastic Test Apparatus (NATA) at Texas A&M University was developed to experimentally test linear and nonlinear aeroelastic behavior. NATA provides a wing mount (herein, we use a rigid NACA 0015 wing section) that provides for movement in two degrees of freedom – pitch and plunge (sometimes referred to as *heave*), as shown schematically in Fig. 1. Stiffness nonlinearity can be introduced in either degree of freedom. For the research, NATA is mounted in a 2’ x 3’ low speed wind tunnel capable of speeds up to 45 m/s.

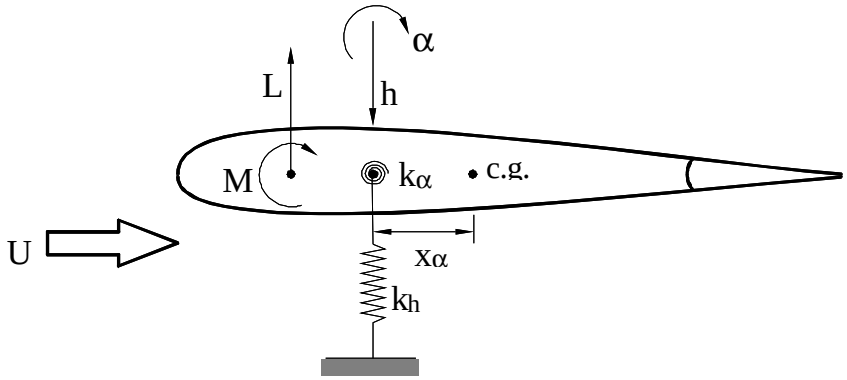

Figure 1. Typical two-dimensional aeroelastic wing model with two degrees of freedom.

Each degree of freedom of the NATA wing is supported by its own set of springs. Plunge motion, which mimics out-of-plane bending motion of the wing, is provided by mounting the wing on a carriage which slides on shafts mounted under the wind tunnel. The motion of the carriage is restricted by springs stretching from the rigid frame of the wind tunnel to a rotating cam. The carriage is attached to the same cam such that its movement is resisted by the springs, as shown in Fig. 2.

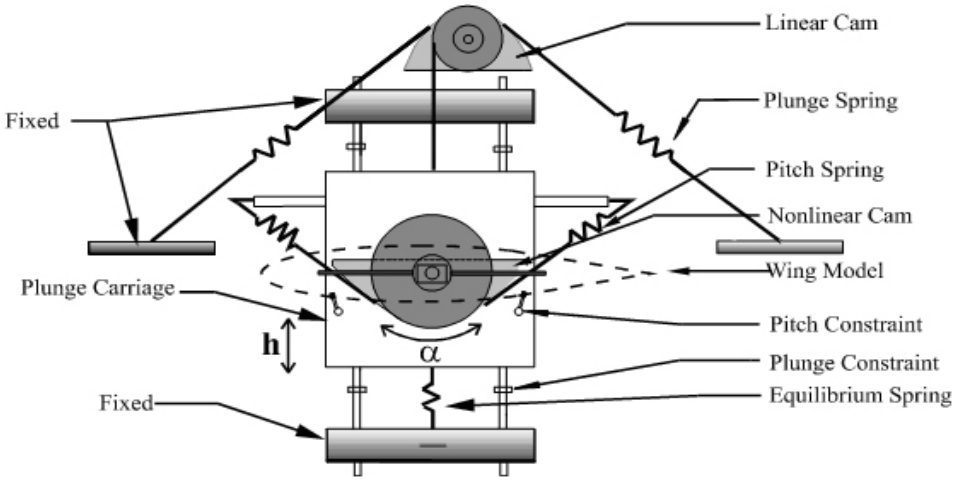

Figure 2. Schematic view of the Nonlinear Aeroelastic Test Apparatus (NATA).

The wing section stands vertically in the wind tunnel, spanning the entire tunnel from top to bottom, as shown in Fig. 3. The wing is attached to a shaft that exits through the tunnel floor and mounts via rotational bearings to the plunge carriage beneath the tunnel. These bearings allow the wing to pitch (rotate), simulating torsional response of the wing. The pitch springs have one end rigidly fixed to the plunge carriage. The other end wraps around a cam on the pitch shaft and attaches to the wing, as shown in Fig. 2.

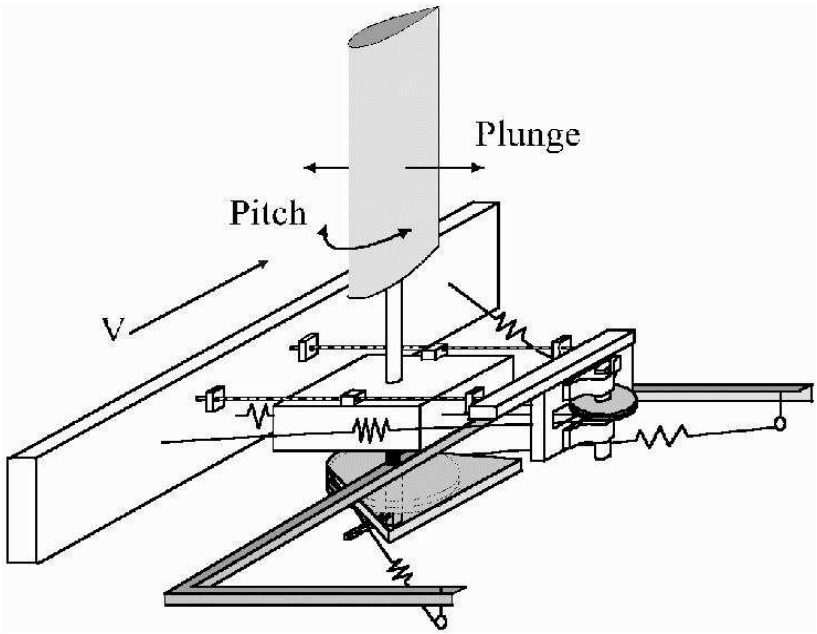

Figure 3. Isometric view of the nonlinear aeroelastic test apparatus.

The shape of the cams in each degree of freedom determines whether the response in that direction will be linear or nonlinear. A circular cam gives a linear spring force while a nonlinear (parabolic shaped) cam will provide a nonlinear stiffening effect. Each degree of freedom can be made linear or nonlinear independently of the other. And, as a consequence of the design, prescribed responses are provided by a specifically tailored cam shape. All tests described herein use a linear plunge cam and a nonlinear pitch cam.

The NES used in the experiments described herein consists of a small 'car' made of aluminum angle stock. The car is connected to NATA through a viscous damper and a nonlinear spring with essential near-cubic stiffness. This spring is created by securing a pair of thin wires in a direction perpendicular to the direction of movement of the NATA and the NES. The wires are mounted such that they have no initial tension and thus no linear spring force component. The arrangement of wires ensures that when NATA or NES moves relative to each other, tension is created in the wires, providing a cubic restoring force. The entire NES assembly attaches to the NATA plunge carriage by a rigid rod. Figure 4 shows NES. The NES car is supported by an aluminum air track that reduces sliding friction in the system. The NES used in experiments with the NATA, along with the air track, is shown in Figs. 5-6 as installed and connected to the NATA plunge carriage.

The pitch and plunge responses of the aeroelastic system are recorded by optical encoders measuring the rotation of the pitch and plunge cams. Free stream velocity inside the wind tunnel is measured using a Pitot probe and an electronic pressure transducer. NES response is measured using an accelerometer. The force applied between the NES and NATA is measured using a force transducer. All of these signals are sent to a data acquisition board and recorded.

The first step in performing experiments with the NATA and the NES is to set the wind tunnel to the desired free stream velocity. Next, initial conditions are given to the NATA and equilibrium at those initial conditions is established. Finally, the system is released and the dynamic response is recorded. All initial conditions used in experiments described herein were non-zero plunge displacements with zero pitch displacement – initial velocities are zero in both pitch and plunge.

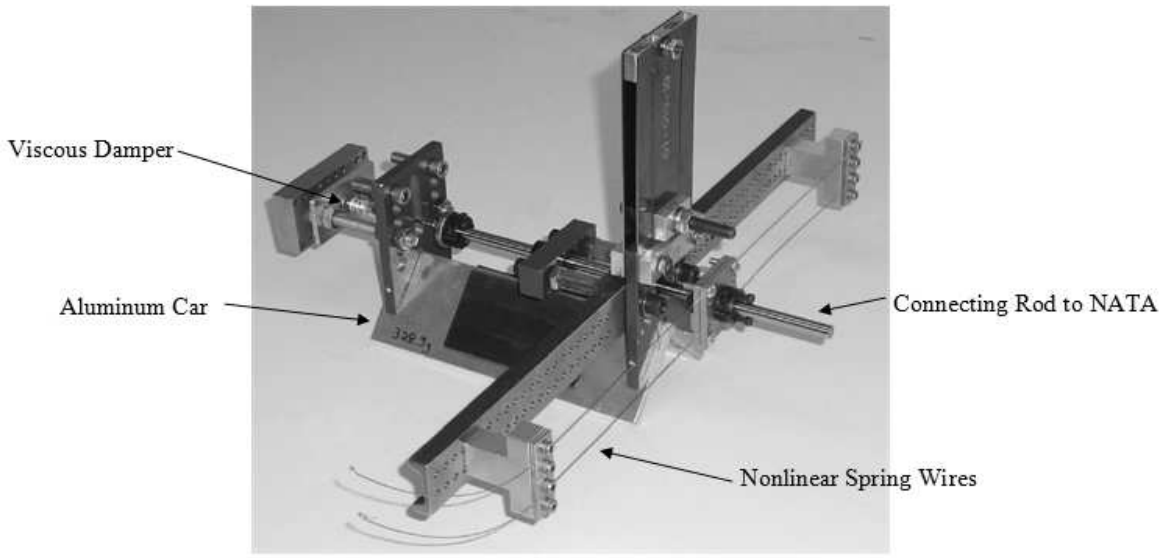

(a)

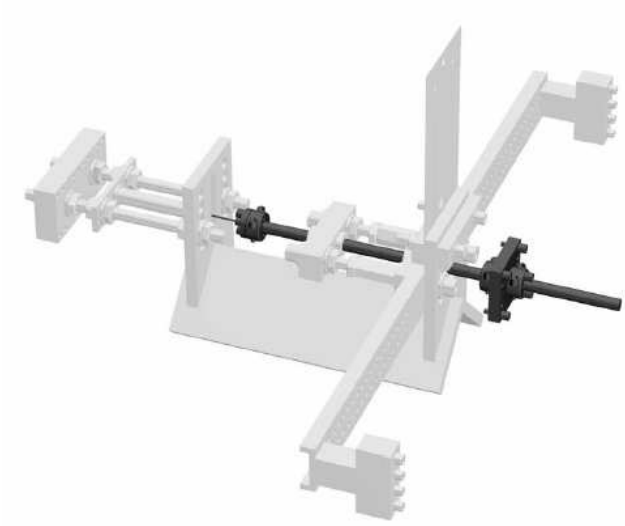

(b)

Figure 4. Nonlinear Energy Sink (NES)[25, 27]: (a) hardware used with NATA; (b) schematic showing mass partition (dark portion moves with wing plunge motion, light portion constitutes NES mass).

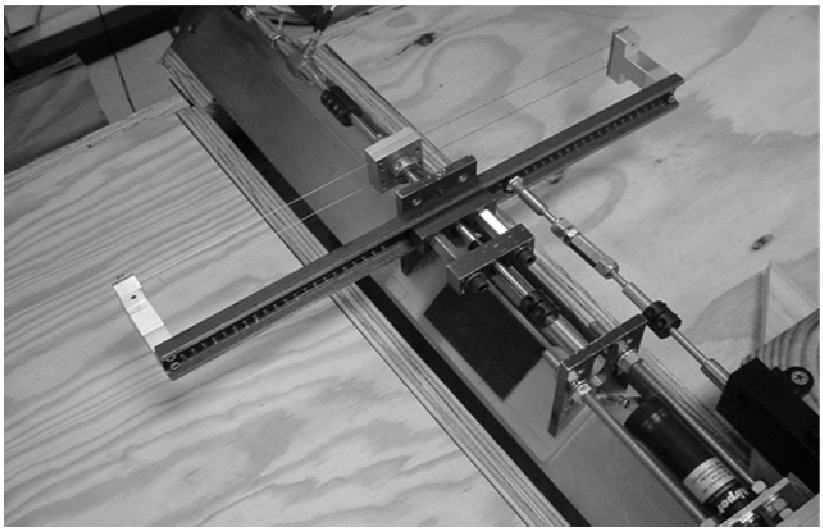

Figure 5. The NES, as used in experiments, rides on the aluminum air track.

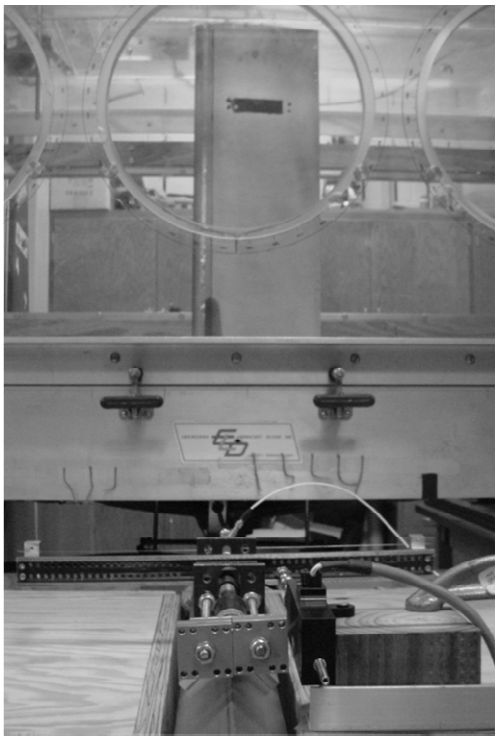

Figure 6. The NES as connected to the NATA.

IV. Equations of Motion

The equations of motion of NATA with wing, but without the NES, are given in Eq. 1:

$$M\begin{Bmatrix}\ddot{h}\\ \ddot{\alpha}\end{Bmatrix}+C\begin{Bmatrix}\dot{h}\\ \dot{\alpha}\end{Bmatrix}+K\begin{Bmatrix}h\\ \alpha\end{Bmatrix}=\begin{Bmatrix}-L\\ M_a\end{Bmatrix}+\begin{Bmatrix}F_c\\ M_c\end{Bmatrix} \tag{1}$$

In Eq. 1, M is a mass matrix, C is a damping matrix that includes a nonlinear kinematic term, and K is a stiffness matrix. These matrices are expressed in terms of the physical parameters of the system in Eqs. 2-4.

$$M = \begin{bmatrix} m_T & m_w r_{cg}\cos\alpha - m_c r_c \sin\alpha \\ m_w r_{cg}\cos\alpha - m_c r_c \sin\alpha & I_\alpha \end{bmatrix} \tag{2}$$

$$C = \begin{bmatrix} c_h & -(m_w r_{cg}\sin\alpha + m_c r_c \cos\alpha)\dot{\alpha} \\ 0 & c_\alpha \end{bmatrix} \tag{3}$$

$$K = \begin{bmatrix} k_h & 0 \\ 0 & k_\alpha(\alpha) \end{bmatrix} \tag{4}$$

The stiffness in pitch is denoted $k_\alpha(\alpha)$ to signify that the nonlinear stiffness is a function of α. The model used to represent k_α is given in Eq. 5.

$$k_\alpha = 8.6031 - 27.67\alpha + 867.15\alpha^2 + 376.64\alpha^3 - 7294.6\alpha^4 \tag{5}$$

This model was created by a least squares fit to measurements of angular displacement of the system and the resulting restoring moment created by the nonlinear pitch cam. The stiffness model given in Eq. 5 and the measured values are plotted versus angular displacement in Fig. 7.

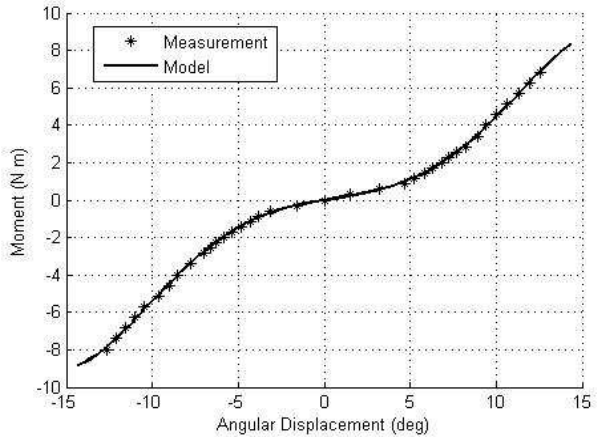

Figure 7. Model and measured stiffness for NATA pitch spring.

Experiments using NATA are conducted at low speeds (typically less than 20m/s) and at very low reduced frequency (typically less than 0.1). The wing section spans the entire wind tunnel so the flow can be considered two-dimensional. For this flow environment, aerodynamic lift and drag can be modeled with quasi-steady aerodynamics. This aerodynamic model has provided very good agreement with NATA experimental results in the past [9, 11-14]. Friction has a significant impact on the dynamic behavior of the NATA system. Both viscous and Coulomb damping appear in Eq. 1 to account for friction in the system.

To account for the presence of the NES, the equations of motion for the NATA are only slightly modified. A term is added to the plunge equation to represent the force the NES exerts on the NATA, F_s. There is no change in the pitch equation since the NES connects only to the plunge carriage – not the wing or rotating shaft. The NATA equations of motion including the NES are given by Eq. 6.

$$M\begin{Bmatrix} \ddot{h} \\ \ddot{\alpha} \end{Bmatrix} + C\begin{Bmatrix} \dot{h} \\ \dot{\alpha} \end{Bmatrix} + K\begin{Bmatrix} h \\ \alpha \end{Bmatrix} = \begin{Bmatrix} -L \\ M_a \end{Bmatrix} + \begin{Bmatrix} F_{ch} \\ F_{c\alpha} \end{Bmatrix} + \begin{Bmatrix} F_s \\ 0 \end{Bmatrix} \tag{6}$$

The equation of motion of the NES is then given by Eq. 7.

$$m_s \ddot{v} = -F_s \tag{7}$$

The force exerted by the NES on the NATA is expressed in terms of the motion of the NES and its physical parameters according to Eq. 8.

$$F_s = c_s\left(\dot{v} - \dot{h}\right) + k_s \left|v - h\right|^{2.8} \operatorname{sgn}(v - h) = 0 \tag{8}$$

The physical parameters for the NATA and NES as configured for all experiments described here are given in Table 1 and Table 2.

Table 1. NATA Parameters

Parameter	Symbol	Value	Units
Wing Mass	m_w	1.645	kg
Pitch Cam Mass	m_c	0.714	kg
Total Plunging Mass	m_T	12.1	kg
Total Pitching Inertia	I_α	$0.04561 + m_w r_{cg}^2$	kg m^2
Wing Mass Offset	r_{cg}	$-b(a+0.18)$	m
Wing Section Semichord	b	0.1064	m
Nondimensional Elastic Axis Location	a	-0.4	--
Pitch Cam Mass Offset	r_c	0.127	m
Viscous Plunge Damping Coefficient	c_h	5.0747	kg/s
Viscous Pitch Damping Coefficient	c_α	0.015	kg m^2/s
Plunge Spring Stiffness	k_h	2537.2	N/m
Pitch Spring Stiffness	k_α	see Eq. 5	N m/rad
Wing Section Span	s	0.6	m

Table 2. NES Parameters

Parameter	Symbol	Value	Units
NES Mass	m_s	1.2	kg
Viscous Damping Coefficient	c_s	1.0	kg/s
Spring Stiffness	k_s	1.6×10^6	N/m$^{2.8}$

V. Experimental Results

Without the NES, the NATA as configured exhibits a Hopf bifurcation at 9.5 m/s, which is the system's linear flutter velocity, V_F. Numerical simulation without Coulomb damping effects shows that the system should experience subcritical LCOs at speeds as low as 4 m/s, as shown on the left view of Fig. 8. However, an effect of Coulomb damping is the elimination of all subcritical behavior. Numerical simulation with Coulomb damping included, as well as the experimental measurements, indicate only supercritical LCO behavior as shown in the bifurcation diagram on the right view of Fig. 8.

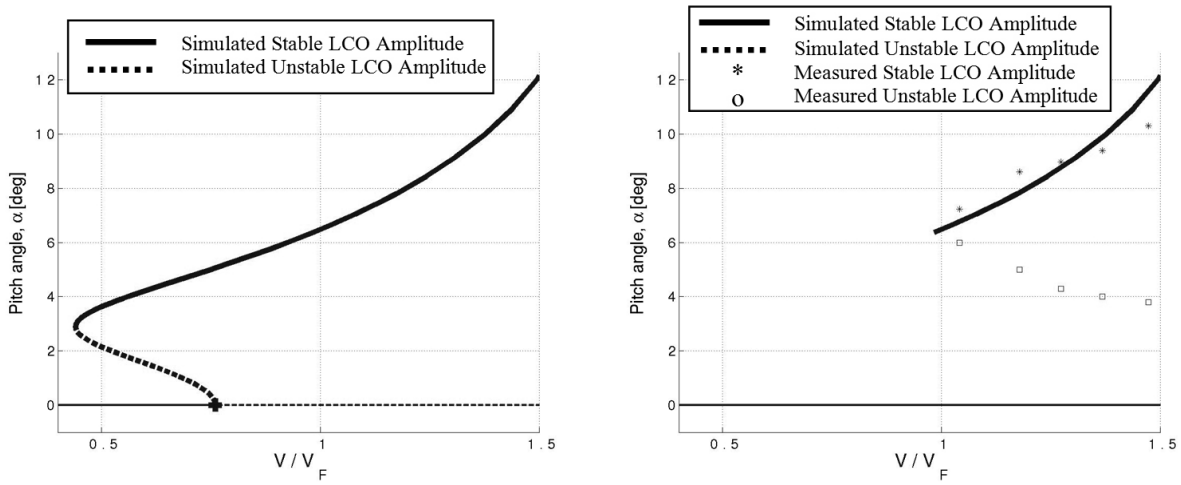

Figure 8. Bifurcation diagrams of stable and unstable LCO amplitudes of pitch response are shown: left view, simulations without Coulomb damping; right view, simulations with Coulomb damping and measured response data.

AUTO2000[32] was employed for the simulated bifurcation analysis in Fig. 8. AUTO2000 is a continuation and bifurcation analysis program for ordinary differential equations. It automates the solution of parameter-dependent systems of equations, including systems whose solutions exhibit periodic phenomena, such as LCOs. The solution set forms a bifurcation diagram; i.e., a smooth curve representing the solution values for the varying system parameter.

To more clearly see the effect of the NES, all NATA experimental velocities discussed are non-dimensionalized by the system's linear flutter velocity, 9.5 m/s, and indicated V^*. Experiments were conducted with the NATA with and without the NES attached, at many different free stream velocities. For each velocity, several initial conditions were tested. All initial conditions were non-zero displacements in plunge with zero pitch displacement and zero pitch and plunge velocity.

The NES dramatically changes the dynamic response of the NATA. Even below the bifurcation point, at $V^* = 0.95$, where the NATA does not exhibit LCOs, the NES causes disturbances to dissipate more quickly, as seen in Fig. 9. The two plots in the right side view show plunge and pitch response of the NATA without the NES caused by a 1.2 cm initial plunge displacement. The two plots on the left side view show pitch and plunge response with the NES and the same initial condition. Figure 9 shows that the NES causes the disturbance to dissipate in almost exactly half the time compared with the unmodified system. The NES also decreases the magnitude of disturbance in the pitch degree of freedom. With the NES attached, the system develops a maximum angular displacement of only 3.2º, compared with 7.1º for the system without the NES.

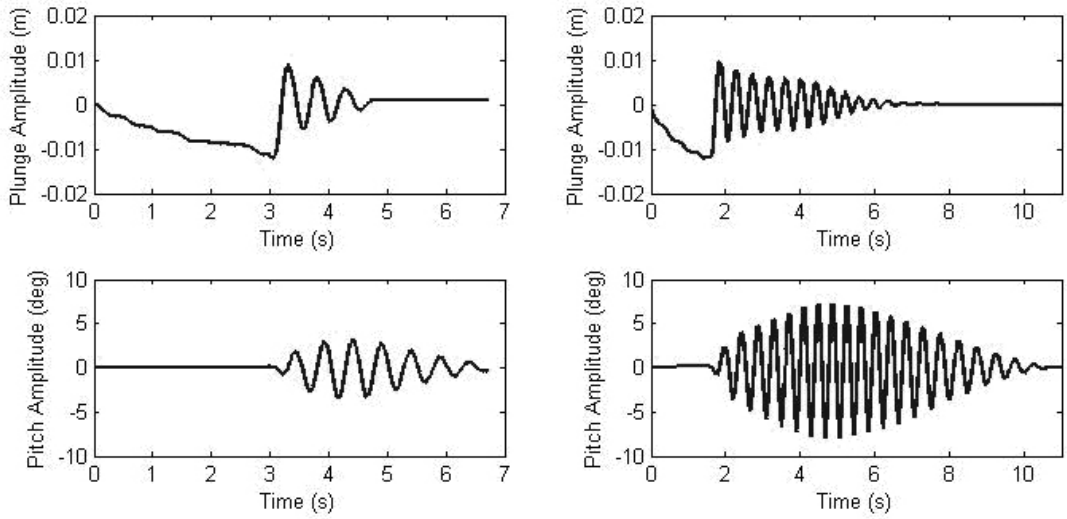

Figure 9. Comparison of the NATA response with the NES (left view) and without the NES (right view); V^* = 0.95, h(0) = 1.2 cm.

When the NES is not present, the NATA develops a LCO above $V^* = 1$. The amplitude of the LCO increases as free stream velocity increases, as shown for the pitch degree of freedom in Fig. 8. The development of the LCO is dependent on the magnitude of the displacement given to the system. For small initial displacements, friction in the system damps out the disturbance before an LCO can develop. The size of the disturbance required to cause a LCO is reduced with increasing free stream velocity. This is reflected through the unstable LCO and is illustrated in Fig. 8; for disturbances above the unstable LCO, motion migrates to a stable LCO with amplitude as shown in Fig. 8. At $V^* = 1.16$, the NATA develops a LCO for plunge displacements greater than 1.1 cm. Figure 10 shows the NATA system response at $V^* = 1.16$ for an initial displacement of 1.2 cm.

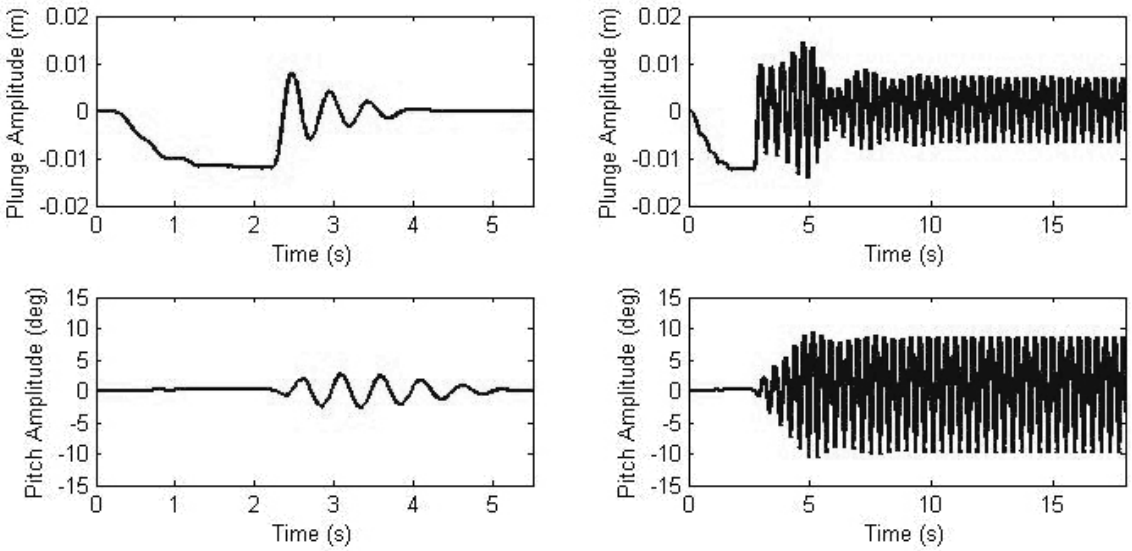

Figure 10. Comparison of the NATA response with the NES (left view) and without the NES (right view); V^* = 1.16, h(0) = 1.2 cm.

Figure 10 shows that the NES does a very good job of suppressing LCO behavior in the NATA at $V^* = 1.16$. The NES is capable of completely suppressing LCOs in the NATA for displacements of up to 1.8 cm at this speed, where only 1.1 cm of displacement is necessary to trigger a LCO in the system without the NES. The suppression is very quick, preventing large pitch displacements from developing.

At V^* = 1.4, only 0.8 cm plunge displacement is required for the NATA to develop a LCO without the NES. With the NES, the system is stabilized for plunge disturbances up to 1.1 cm, an increase of 38%. With plunge disturbances greater than 1.1 cm, the system develops LCOs even with the NES. However, as can be seen in Fig. 11, for V^* = 1.4 and initial displacement of 1.2 cm, the amplitude of both pitch and plunge oscillation is significantly smaller with the NES: 42% lower in plunge and 20% lower in pitch.

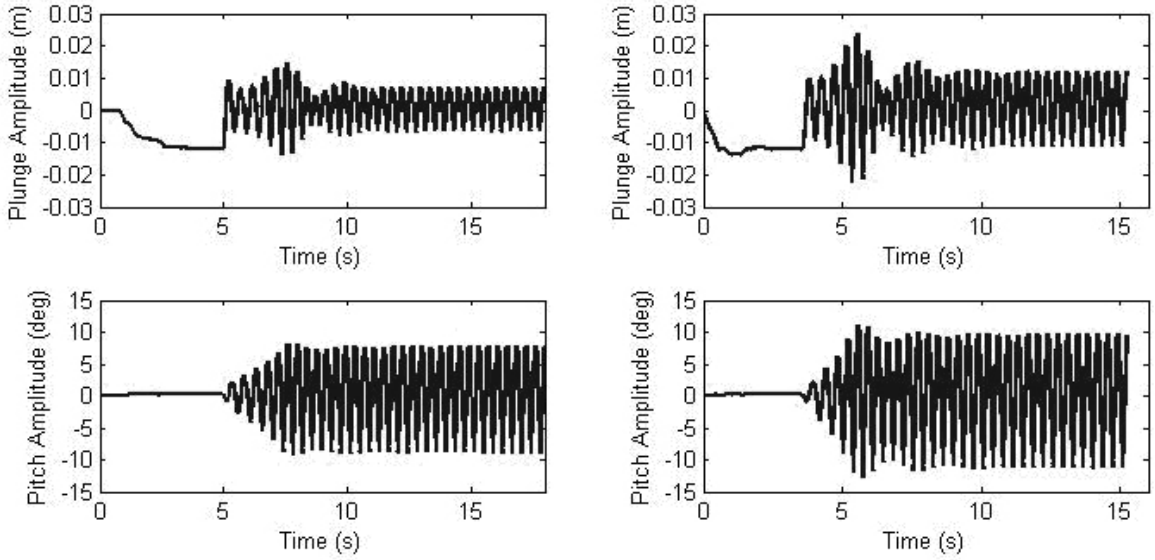

Figure 11. Comparison of the NATA system response with the NES (left view) and without the NES (right view); *V = 1.4, h(0) = 1.2 cm.**

VI. Conclusion

We have demonstrated the Nonlinear Energy Sink as a passive method for suppressing or reducing limit cycle oscillations in an aeroelastic system. Experimental results show that nonlinear energy pumping is capable of irreversibly transferring and dissipating vibrational energy from the aeroelastic system. Results at various flow speeds show that the Nonlinear Energy Sink can extend the stable operational envelope of an aeroelastic system that possesses limit cycle oscillations. At higher vehicle velocities the system may experience limit cycle oscillations, however the amplitude of oscillation is significantly reduced due to the Nonlinear Energy Sink.

References

[1]Denegri, C. M., Jr., "Limit Cycle Oscillation Flight Test Results of a Fighter with External Stores," *Journal of Aircraft*, Vol. 37, No. 5, 2000, pp. 761-769.

[2]Bunton, R. W., and Denegri, C. M., Jr., "Limit Cycle Oscillation Characteristics of a Fighter Aircraft," *Journal of Aircraft*, Vol. 37, No. 5, 2000, pp. 916-918.

[3]Croft, J., "Airbus Elevator Flutter: Annoying or Dangerous?" *Aviation Week and Space Technology*, Vol. 155, Issue 9, 2001, p. 41.

[4]Dowell, E., Edwards, J., and Strganac, T., "Nonlinear Aeroelasticity," *Journal of Aircraft*, Vol. 40, No. 5, 2003, pp. 857-874.

[5]Cunningham, A. M., Jr., "The Role of Nonlinear Aerodynamics in Fluid-Structure Interactions," AIAA Paper 98-2423, 1998.

[6]Hartwich, P. M., Dobbs, S. K., Arslan, A. E., and Kim, S.C., "Navier-Stokes Computations of Limit Cycle Oscillations for a B-1-Like Configuration," AIAA Paper 2000-2338, 2000.

[7]Chen, P. C., Sarhaddi, D., and Liu, D. D., "Limit Cycle Oscillation Studies of a Fighter with External Stores," *39th AIAA Structures, Structural Dynamics, and Materials Conference*, AIAA Paper 98-1727, 1998.

[8]Gilliatt, H. C., Strganac, T. W., and Kurdila, A. J., "An Investigation of Internal Resonance in Aeroelastic Systems," *Nonlinear Dynamics*, Vol. 31, 2003, pp. 1-22.

[9]Thompson, D. E., and Strganac, T. W., "Store-Induced Limit Cycle Oscillations and Internal Resonances in Aeroelastic Systems," *41st AIAA Structures, Structural Dynamics, and Materials Conference*, AIAA Paper 2000-1413, 2000.

[10]Tang, D. and Dowell, E., "Experimental and Theoretical Study on Aeroelastic Response of High-Aspect-Ratio Wings," *AIAA Journal*, Vol. 39, No. 8, 2001, pp. 1430-1441.

[11]O'Neil, T., "Nonlinear Aeroelastic Response – Analyses and Experiments," *AIAA Aerospace Sciences Meeting and Exhibit*, AIAA Paper 96-0014, 1996.

[12]O'Neil, T., Gilliatt, H., and Strganac, T., "Investigations of Aeroelastic Response for a System with Continuous Structural Nonlinearities," *37th AIAA Structures, Structural Dynamics and Materials Conference*, AIAA Paper 96-1390, 1996.

[13]Sheta, E. F., Harrand, V. J., Thompson, D. E., and Strganac, T. W., "Computational and Experimental Investigation of Limit Cycle Oscillations in Nonlinear Aeroelastic Systems," *AIAA Structures, Structural Dynamics, and Materials Conference*, AIAA Paper 2000-1399, 2000.

[14]Thompson, D. E., "Nonlinear Analysis of Store Induced Limit Cycle Oscillations," M.S. Thesis, Texas A&M University, 2001.

[15]Ko, J., Strganac, T. W., and Kurdila, A. J., "Adaptive Linearization for the Control of a Typical Wing Section with Structural Nonlinearity," *Nonlinear Dynamics*, No. 18, 1999, pp. 289-301.

[16]Ko, J., Kurdila, A. J., and Strganac, T. W., "Nonlinear Control of a Prototypical Wing Section with Torsional Nonlinearity," *Journal of Guidance, Control, and Dynamics*, Vol. 20, No. 6, 1997, pp. 1181-1189.

[17]Block, J. J. and Strganac, T. W., "Applied Active Control for a Nonlinear Aeroelastic Structure," *Journal of Guidance, Control, and Dynamics*, Vol. 21, No. 6, 1998, pp. 838-845.

[18]Platanitis, G., and Strganac T. W., "Control of a Nonlinear Wing Section Using Leading- and Trailing-Edge Surfaces," *Journal of Guidance, Control, and Dynamics*, Vol. 27, No. 1, 2004, pp. 52-58.

[19]Vakakis, A. F. and Gendelman, O., "Energy Pumping in Nonlinear Mechanical Oscillators: Part II – Resonance Capture," *Journal of Applied Mechanics*, Vol. 68, January 2001, pp. 42-48.

[20]Vakakis, A. F., McFarland, D. M., Bergman, L. A., Manevitch, L. I. and Gendelman, O., "Isolated Resonance Captures and Resonance Capture Cascades Leading to Single- or Multi-Mode Passive Energy Pumping in Damped Coupled Oscillators," ASME *Journal of Vibration and Acoustics*, Vol. 126, No. 2, 2004, pp. 235–244.

[21]O. Gendelman, L. I. Manevitch, A. F. Vakakis, R. M'Closkey, 2001, "Energy Pumping in Nonlinear Mechanical Oscillators: Part I-Dynamics of the Underlying Hamiltonian Systems," *Transactions of the ASME, Journal of Applied Mechanics*, Vol. 68, pp. 34-41.

[22]Lee, Y. S., Kerschen, G., Vakakis, A. F., Panagopoulos, P., Bergman, L., and McFarland, D. M., "Complicated Dynamics of a Linear Oscillator with a Light, Essentially Nonlinear Attachment," *Physica D*, Vol. 204, 2005, pp. 41-69.

[23]Kerschen, G., Lee, Y. S., Vakakis, A. F., McFarland, D. M. and Bergman, L. A., "Irreversible Passive Energy Transfer in Coupled Oscillators with Essential Nonlinearity," SIAM Journal on Applied Mathematics, submitted for publication.

[24]Lee, Y. S., Vakakis, A. F., Bergman, L. A. and McFarland, D. M., "Suppression of Limit Cycle Oscillations in the van der Pol Oscillator by Means of Passive Nonlinear Energy Sinks (NESs)," Structural Control and Health Monitoring, submitted for publication.

[25]Lee, Y. S., Vakakis, A. F., Bergman, L. A., McFarland, D. M. and Kerschen, G., "Triggering Mechanisms of Limit Cycle Oscillations due to Aeroelastic Instability," Journal *of Fluids and Structures*, submitted for publication.

[26]Lee, Y. S., Kerschen, G., Vakakis, A. F., McFarland, D. M. and Bergman, L. A., "Suppression of Limit Cycle Oscillations with a Nonlinear Energy Sink: Theoretical Basis," *AIAA SDM 2006*, submitted for publication.

[27]Kowtko, J. J., "Experiments with Nonlinear Energy Sinks: A Novel Approach to Vibrational Energy Dissipation," M.S. Thesis, University of Illinois at Urbana-Champaign, 2005.

[28]Vakakis, A. F., Manevitch, L. I., Gendelman, O., and Bergman, L., "Dynamics of Linear Discrete Systems Connected to Local, Essentially Non-Linear Attachments," *Journal of Sound and Vibration*, Vol. 264, 2003, pp. 559-577.

[29]McFarland, D. M., Bergman, L. A., Vakakis, A. F., "Experimental Study of Non-Linear Energy Pumping Occurring at a Single Fast Frequency," *International Journal of Nonlinear Mechanics*, Vol. 40, 2005, pp. 891-899.

[30]McFarland, D. M., Kerschen, G., Kowtko, J. J., Bergman, L. A. and Vakakis, A. F., "Experimental Investigation of Targeted Energy Transfers in Strongly and Nonlinearly Coupled Oscillators," Journal of the Acoustical Society of America, submitted for publication.

[31]Kerschen, G., Vakakis, A. F., Lee, Y. S., McFarland, D. M., Kowtko, J. J. and Bergman, L. A., "Energy Transfers in a System of Two Coupled Oscillators with Essential Nonlinearity: 1:1 Resonance Manifold and Transient Bridging Orbits," Nonlinear Dynamics, submitted for publication.

[32]Doedel E. J., Paffenroth, R. C., Champneys, A. R., Fairgrieve, T. F., Kuznetsov, Y. A., Sandstede, B., and Wang, X. J., "AUTO2000: Continuation and Bifurcation Software for Ordinary Differential Equations," Technical Report, California Institute of Technology, 2002.